

Amphotericin B Binds to Amyloid Fibrils and Delays Their Formation: A Therapeutic Mechanism?[†]

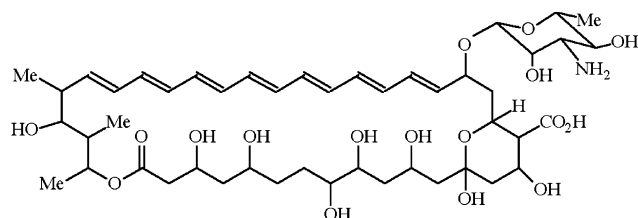
Scott C. Hartsel* and Theodore R. Weiland

Department of Chemistry, University of Wisconsin—Eau Claire, Eau Claire, Wisconsin 54702-4004

Received October 21, 2002; Revised Manuscript Received December 23, 2002

ABSTRACT: The membrane-active antifungal agent amphotericin B (AmB) is one of the few agents shown to slow the course of prion diseases in animals. Congo Red and other small molecules have been reported to directly inhibit amyloidogenesis in both prion and Alzheimer peptide model systems via specific binding. We propose that it is possible that AmB may act similarly to physically prevent conversion of the largely α -helical prion protein (PrP) to the pathological β -sheet aggregate protease-resistant isoform (PrP_{res}) in prion disease and by analogy prevent fibrillization in amyloid diseases. To assess whether AmB is capable of binding specifically to amyloid fibrils as does Congo Red, we have used the insulin fibril and A β 25–35 amyloid model fibril system. We find that AmB does bind strongly to both insulin ($K_d = 1.1 \mu\text{M}$) and A β 25–35 amyloid ($K_d = 6.4 \mu\text{M}$) fibrils but not to native insulin. Binding is characterized by a red-shifted AmB spectrum indicative of a more hydrophobic environment. Thus AmB seems to have a complementary face for amyloid fibrils but not the native protein. In addition, AmB interacts specifically with Congo Red, a known fibril-binding agent. In kinetic fibril formation studies, AmB was able to significantly kinetically delay the formation of A β 25–35 fibrils at pH 7.4 but not insulin fibrils at pH 2.

Amphotericin B (AmB) is a widely used membrane-active antifungal drug which also shows a remarkable breadth of additional activities (1). For example, it has antiprotozoal



Amphotericin B

(2), antiviral (3), and indirect antimicrobial activity through immune stimulation (4, 5). Most intriguing are reports of the antiprion activity of AmB and its derivatives (6). In fact, amphotericin B (AmB) and its derivatives have been shown to be among the very few agents which can slow the course of prion disease in animal models (7, 8). It is currently unclear as to what the mechanism of action could be, but both direct and indirect blockage of prion PrP_{res} propagation and immune stimulation have been proposed (9).

Transmissible spongiform encephalopathies (TSE) are neurodegenerative diseases which include Creutzfeldt–Jacob disease (CJD) in humans, scrapie in sheep, and chronic wasting disease (CWD) in deer and elk. The causative agent in these diseases is prions, proteinaceous infectious particles,

which can be genetic, acquired, or sporadic. There are over a dozen amyloid diseases, including Alzheimer's disease (AD) and familial amyloidotic polyneuropathy. These are also neurodegenerative diseases which are mainly genetic or sporadic but recently have shown to be transmissible under some circumstances (10). Prions and amyloid diseases have many features in common. Chiefly, they both involve protein misfolding events which can induce other proteins to misfold into largely β -sheet fibrillar or oligomeric isoforms (11, 12). These structures seem to be the key to the disease pathogenesis by various proposed mechanisms (13–15).

There are currently no approved human chemotherapies for these diseases other than relief of secondary effects (16) though vaccines still look promising (17). Inhibition of fibril growth via binding of small specific ligands has been investigated as a possible therapeutic approach for amyloid/prion diseases (18–21). The polyol region of AmB suggests that it could be an effective hydrogen bond donor/acceptor and may be able to terminate and/or stabilize the β -sheet structure of a growing amyloid fibril or oligomer as has been suggested for alternating *N*-methyl peptides and the dye Congo Red (CR) (21). AmB has the further advantage of being a well-characterized drug which is already widely available and has many newer low-toxicity pharmaceutical preparations (1). We hypothesize that AmB may exert its antiprion effect by selectively binding to β -sheet-rich protein fibrils, isoforms, or oligomers and preventing or slowing formation, nucleation, and propagation.

We have investigated this proposed binding interaction using the low-pH bovine insulin amyloid fibril and the A β 25–35 model systems since there seems to be a nearly universal structure for misfolded amyloid proteins including

[†] Supported by the NSF-RUI program (S.C.H.) and the Leoba Hogan Scientific Research Scholarship (T.R.W.).

* To whom correspondence should be addressed. Fax: (715) 836-2380. E-mail: hartsec@uwec.edu.

prions (22). The A β 25–35 peptide, which is the among the most amyloidogenic stretches of the A β 1–42 sequence associated with AD, shows sequence and chemical similarities to the critical hydrophobic core sequence of the prion protein, PrP 106–126 (23). A specific binding interaction of AmB was observed for both insulin and A β 25–35 fibrils as quantitated by a red shift of the monomer absorbance and disassembly of the AmB oligomer. No significant binding to the native insulin structure was observed. AmB also binds to Congo Red and thus seems to have a complementary surface both for Congo Red and for amyloid fibrils. In the insulin fibril seeding model at pH 2.0, AmB did not inhibit fibrillogenesis kinetics, but in the more active A β 25–35 system at pH 7.4, AmB was able to significantly delay fibrillogenesis.

MATERIALS AND METHODS

Materials. Purified amphotericin B, FMOC/OPfp amino acid derivatives, Congo Red, and bovine insulin (I-5500, 0.5% Zn) were obtained from Sigma Chemical Co. (St. Louis, MO). Amphotericin B was prepared in DMSO at a concentration of 1 mM and quantitated by removing aliquots into 100% MeOH using the extinction coefficient of 150000 at 406 nm. The standard Congo Red solution for all assays was prepared in Congo Red (CR) buffer (0–25 μ M Congo Red, 0.15 M NaCl, 5 mM KH₂PO₄, pH 7.4).

Synthesis of A β 25–35. The A β 25–35 undecapeptide, GSNKGAIIGLM, was synthesized using standard FMOC/OPfp chemistry with a Protein Technologies PS3 peptide synthesizer. The peptide was analyzed and purified in the laboratory using reversed-phase HPLC (POROS R2 media). The peptide was stored at –70 °C as a lyophilized powder. The peptide composition and purity were confirmed using MALDI-MS.

Formation of Fibrils. Insulin fibrils were produced essentially as described in ref 24. Briefly, a fresh insulin solution in deionized water was brought to pH 2.0 with HCl. The insulin solution was then subjected to seven freeze/thaw/heating steps, which involved the use of liquid nitrogen and a water bath at 92 °C. The solution was sonicated with a probe sonicator for 1 min prior to use. A β 25–35 fibrils were produced as described in Klunk et al. (25). Briefly, a fresh A β 25–35 solution at 1 mM was made up in phosphate-buffered saline (PBS, 155 mM NaCl, 7 mM Na₂HPO₄, 3 mM KH₂PO₄, pH 7.4) and was incubated at 22 °C for 48 h with stirring. Within 3 h solutions were visibly cloudy and contained amyloid fibrils as measured by Congo Red binding. The solutions were stored at 4 °C when not in use. The presence of characteristic fibrils was confirmed with electron microscopy using a 3% uranyl acetate negative stain.

Fibril Binding Assay for AmB. A β 25–35 and insulin fibril solutions were titrated with 0–50 μ M AmB from DMSO solutions. Scans were taken from 300 to 500 nm with a Cary 50 spectrophotometer. The concentration of bound AmB was estimated using an absorption coefficient previously determined from the spectrum of 5 μ M AmB in the presence of increasing amounts of insulin fibrils (5–100 μ M). The hyperbolic fit to the 0–0 absorption maxima value at 418 nm provided the absorption coefficient of $\epsilon = 97500$. The amount of the AmB/fibril complex was estimated using this value and was measured at 418 nm for insulin fibrils and

420 nm for A β 25–35 fibrils. The absorption coefficient was assumed to be the same for both fibril preparations.

The binding data were fitted to a function, taking into account the effect of receptor depletion when ligand concentration is of the same order of magnitude as receptor concentration from Ellison (26) and taking into account the increasing absorbance “tail” of AmB (a linear function):

$$[\text{RL}] = \frac{(K_d + R_T + L_T) - \sqrt{(K_d + R_T + L_T)^2 - 4R_T L_T}}{2} + \text{NL}_T$$

where [RL] is the receptor–ligand complex, K_d is the dissociation constant, R_T is the total receptor (insulin or A β 25–35), and L_T is the total ligand (AmB). The function was fitted using SigmaPlot.

Kinetic Fibril Formation Assay: (A) Insulin. It was necessary to introduce a seed from preexisting fibril to overcome the lengthy lag time in the insulin/fibril system (24). A fibril “seed” consisting of 0.085 mg/mL fibrillar insulin was added to a 2 mg/mL solution of native bovine insulin at pH 1.6, 0.1 M NaCl, and 22 °C as described in ref 24. In one experiment 15 μ M AmB was added to the mixture at the outset. From these tubes of insulin, 100 μ L aliquots were taken every 15 min. These aliquots were added to 3 mL of 25 μ M CR and probe sonicated for 30 s before being scanned from 300 to 600 nm. At the final concentration of AmB (0.5 μ M), an AmB–CR spectral interference was considered minimal as shown by AmB/CR titration data.

(B) A β 25–35 Assay. A β 25–35 fibrillization kinetics were assayed in a similar manner, except that PBS was used for the 2 mg/mL solution of fresh A β 25–35 peptide. Because of A β 25–35’s rapid fibril-forming ability, no seed was needed. AmB concentrations used in the fibril formation inhibition studies were 7.5 and 15 μ M.

RESULTS

AmB Fibril Binding: Absorption Spectra. The amphotericin B spectrum in aqueous solution at concentrations >1 μ M consists of a combination of two principal species. These are a monomeric form consisting of the typical polyene vibrational structure (aqueous absorption maxima at ca. 409, 385, 362, and 345 nm) and a self-associated form(s), typically a single blue-shifted band at 330–340 nm. Upon association with 30 μ M (in insulin) fibrillar insulin, the self-associated form is nearly eliminated as the equilibrium shifts toward a protein-bound monomeric form with blue-shifted absorption maxima at 418, 392, 374, and 354 nm (Figure 1). From a titration of a fixed amount of AmB with increasing concentrations of sonicated fibrils an extinction coefficient of 95700 was estimated for the AmB/fibril complex. AmB (5 μ M) with 5–50 μ M native insulin shows no spectral shift or aggregate dissociation, indicating a specific interaction of monomeric AmB with insulin fibrils. AmB also interacted with synthetic A β 25–35 fibrils to give similar protein-bound spectral features with the 0–0 vibronic maximum slightly more red shifted to 419–420 nm. The data clearly show that the amino acid sequence is unimportant in AmB binding since there is virtually no increase in the 418 nm band in the presence of native insulin. Though the sample size is small, these data suggest that AmB is binding to a common

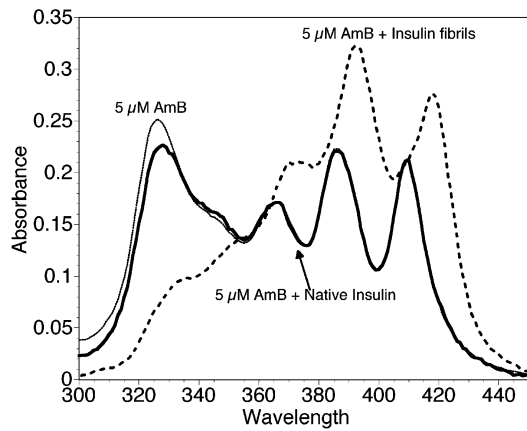


FIGURE 1: Spectroscopic changes in AmB upon binding to insulin fibrils. Insulin fibrils were prepared by incubation at pH 2.0. These fibrils were sonicated and added to a PBS buffer at pH 7.4 with 5.0 μM AmB from a 1 mM AmB/DMSO stock solution and incubated for 5 min at 22 $^{\circ}\text{C}$. The aqueous AmB (light line) and AmB + 30 μM native insulin solutions (heavy line) exhibit nearly identical spectra, consistent with the coexistence of a self-aggregated species with a single band at ~ 328 nm and a typical AmB aqueous monomer with the principal 0–0 transition at 409 nm and other transitions at 386, 366, and 344 nm. In the presence of 30 μM insulin fibrils (dashed line) there is a near disappearance of the aqueous self-associated form replaced by a new red-shifted (418, 392, 373, 350 nm) protein-bound monomeric AmB species.

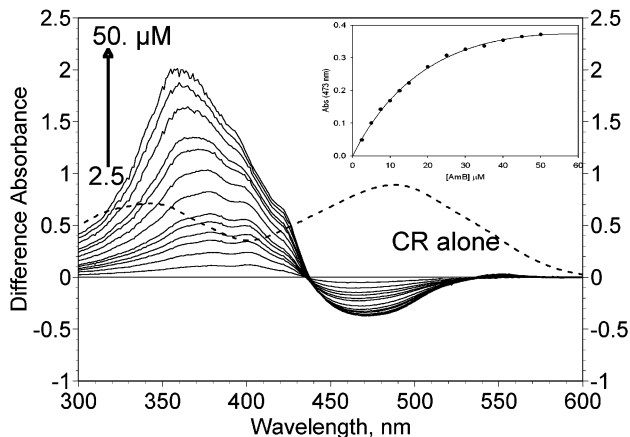


FIGURE 2: Difference spectra of the interaction of 25 μM Congo Red to varying amounts of AmB. A 25 μM Congo Red solution was incubated in CR buffer at 37 $^{\circ}\text{C}$ for 5 min with AmB added from a 1.0 mM DMSO stock solution. 25 μM CR without AmB was the baseline (dashed line) which was subtracted from all of the other spectra to produce the difference. The isosbestic points at 440 and 535 nm suggest a simple two-species transition. The inset of a plot of the CR absorbance loss at 473 nm fitted to a hyperbolic function suggests a saturable interaction between CR and AmB.

fibril structural motif rather than specific amino acid residues much as the fibril-specific azo dye Congo Red.

Since AmB interacted specifically with fibrils, it was of interest to determine whether it also interacted with Congo Red and could possibly interfere with fibrillization assay readings. Figure 2 shows the result of increasing [AmB] on a fixed (25 μM) Congo Red aqueous solution. As demonstrated by the saturable loss of CR absorbance at 470 nm (see inset) and the slight increase at 550 nm, AmB and CR do directly interact. The isosbestic points suggest a clean two-species interaction. The low final concentration of AmB (< 0.5 μM) and the much higher concentration of CR (25

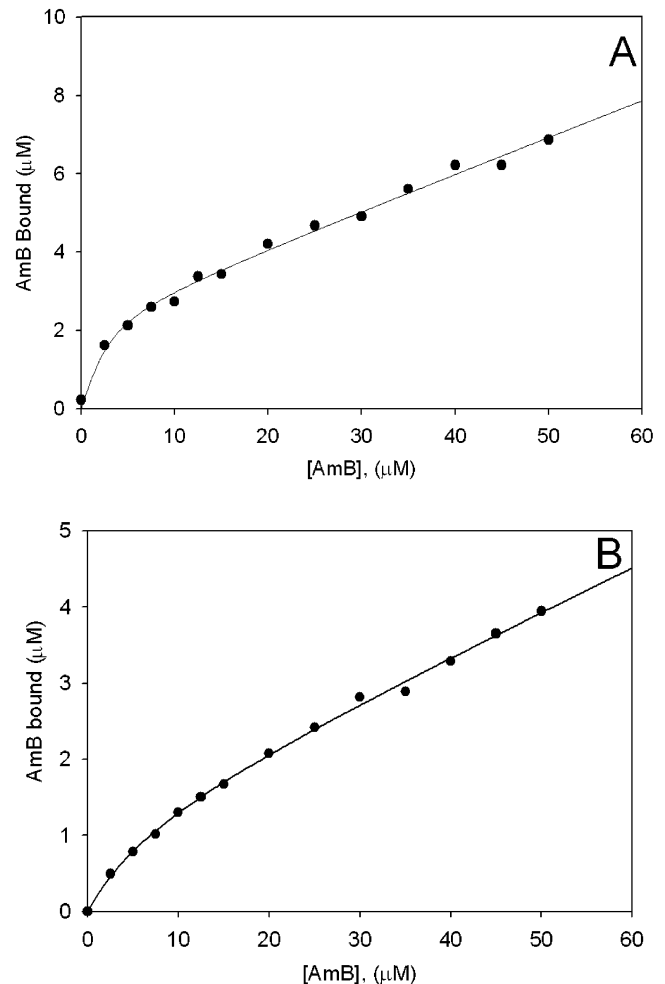


FIGURE 3: Titration of insulin and $\text{A}\beta$ 25–35 fibrils with AmB. Amphotericin binding was fitted to a modified hyperbola with a linear component. Panels: (A) insulin fibrils; (B) $\text{A}\beta$ 25–35 fibrils.

μM) in the fibril kinetic assay suggest that this interaction will not cause significant spectroscopic interference.

Determination of $\text{A}\beta$ 25–35 and Insulin Fibril Apparent AmB Dissociation Constants. We used 5 μM insulin and 25 μM $\text{A}\beta$ 25–35 fibrils for binding titration with AmB in light of the 51-residue insulin versus 11 amino acid residue $\text{A}\beta$ 25–35 difference between the systems. Panels A and B of Figure 3 show the curves generated using the protein-bound AmB absorbance to determine the concentration of the AmB/amyloid complex; 418 nm was used as the absorption maximum for the insulin fibrils versus 420 nm for the $\text{A}\beta$ 25–35. This difference was due to the slight differences in the A_{max} of the two species and also to the larger free AmB interference with the $\text{A}\beta$ 25–35 system, since higher [AmB] was required to approach binding saturation. The curves were fitted to a modified hyperbola with a linear component due to the increasing contribution of the free AmB absorbance tail. It should be noted that “free AmB” is merely a term to indicate non-protein-bound AmB. In reality, at the concentrations used, AmB was largely or entirely in the oligomeric self-associated state as introduced (27, 28). However, AmB was designated as the ligand for these calculations. Even though AmB and $\text{A}\beta$ 25–35 monomers have nearly the same molar mass, the spectra indicate that AmB has dissociated into a bound monomeric form of AmB (a four-band polyene spectrum) and the $\text{A}\beta$ 25–35 is a high molecular mass

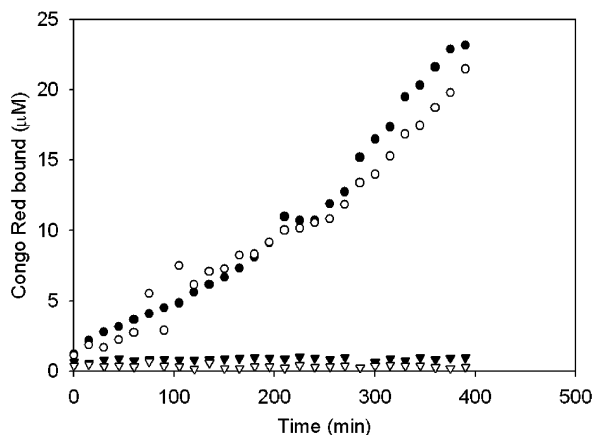


FIGURE 4: Kinetics of fibril growth for 2 mg/mL bovine insulin at pH 2.0 as measured by CR binding in 25 μ M CR buffer. Filled triangles represent unseeded insulin and open triangles 15 μ M AmB alone, open circles are 15 μ M AmB + fibril seeds, and filled circles are fibril seeds alone. Under these conditions AmB neither prevented nor promoted fibrillization.

fibrillar supramolecular complex (29, 30). Thus the amyloid structure more closely resembles the traditional picture of a multisite “receptor”. There is no evidence for similar kinetic reversibility of fibrils (24) under these conditions, and so we consider the receptor to be unchangeable.

Quantitatively, AmB has a K_d of 1.1 μ M for insulin fibrils and 6.4 μ M for $A\beta$ 25–35. In addition, the data indicate that there is a saturation of about 1 molecule of AmB/2 insulin “monomers” in the fibril and about 1 AmB/20 of the $A\beta$ 25–35 peptide monomers. Since the fraction of protein in a fibrillar form is unknown for these systems, the number of AmB binding sites should be regarded as tentative.

Kinetics of Fibril Formation. Figure 4 shows the results of kinetic fibril formation studies on the low-pH (2.0) insulin system. In agreement with previous studies, no appreciable fibrillogenesis occurred over a 400 min time frame in the absence of a seed from mature insulin fibrils (24). In the presence of a seed, the fibrils began to form immediately. According to our hypothesis, AmB could bind to and prevent a seed from nucleating fibrillogenesis and/or could inhibit the process by binding to existing fibrils and arresting further growth. AmB was preincubated with fibrils at 100 μ M, and subsequently the fibrillogenesis mixture was incubated in the presence of 15 μ M AmB. This treatment did not delay the fibrillogenesis process (Figure 4). As a control, 15 μ M AmB was added to an unseeded mixture and failed to promote fibrillogenesis by itself.

Figure 5 shows the results of kinetic fibril formation studies on the pH 7.4 $A\beta$ 25–35 peptide system. $A\beta$ 25–35 is one of the most toxic and most fibrillogenesis-prone peptides contained within the amyloid precursor protein (31, 32). In the absence of added seed, this peptide rapidly forms fibrils after dissolving the lyophilized powder as monitored by CR binding. There is no discernible lag time and the typical half-time of fibrillogenesis is 15–20 min. Seeding by the same protocol as above does not enhance this rate. Adding AmB to the freshly dissolved peptide, however, does have a profound effect on the lag time: 45 min at 7.5 μ M AmB and 150 min at 15 μ M. DMSO alone at the concentrations added from the stock AmB solution did not slow the fibrillogenesis.

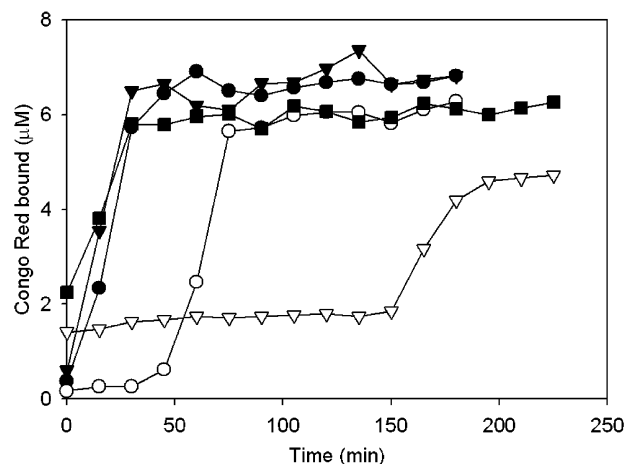


FIGURE 5: Kinetics of fibril growth for 2 mg/mL $A\beta$ 25–35 in PBS at pH 7.4 as measured by CR binding in 25 μ M CR buffer. Filled triangles represent unseeded $A\beta$ 25–35, filled circles are seeded (as for insulin) $A\beta$ 25–35, open circles are $A\beta$ 25–35 incubated with 7.5 μ M AmB, filled squares are a different $A\beta$ 25–35 preparation with unseeded control, and open triangles are the same $A\beta$ 25–35 preparation in the presence of 15 μ M AmB. In both cases AmB significantly delayed the onset of unseeded fibrillization; however, points taken after 12 h indicate the ultimate extent of fibrillization was unaffected.

DISCUSSION

The spectra in Figure 1 and the subsequent binding curves in Figure 3 suggest a specific saturable binding of AmB to amyloid fibrils produced from insulin and $A\beta$ 25–35. On the basis of results of AmB association with serum albumin, it is likely that the “bound” spectra correspond to a nonaqueous protein binding site (33). It is possible that AmB could be binding less specifically to aggregates by hydrophobic interactions, but we feel this is not the case for several reasons. First, $A\beta$ 25–35 is not an extremely hydrophobic peptide overall with an expected net charge of +1 and an Asn, Lys, and Ser residue and three Gly residues. It does, however, have a significant hydrophobic segment (the last five amino acids, IIGLM). The saturability (the hyperbolic component in Figure 3) and the time dependence of the binding paralleling fibril formation (assessed via CR binding) suggest a specific binding to the amyloid structures rather than a precipitate. The specificity of insulin fibril vs native binding suggests a strong preference for the amyloid β -structure rather than simply hydrophobic amino acids. In addition, the specific interaction of AmB with CR (Figure 2) suggests a complementary face to amyloid. Previous diffraction studies of a yeast prion peptide GNNQQNY fibrils suggest a parallel β -sheet thickness of about 22.6 \AA (34). Other model studies of $A\beta$ fibrils suggest a thickness of about 30 or 40 \AA for individual antiparallel β -strands (35, 36). These numbers fit well with the expected length of AmB monomers of 25–30 \AA .

The clean isosbestic point in the spectral series of AmB and Congo Red indicates a simple two-species transition (Figure 2). Since AmB is mostly in the self-associated state at $>1 \mu$ M, it is possible that CR is binding and intercalating into this regular AmB aggregate as it does into amyloid fibrils. Alternatively, it could be causing dissociation of the AmB supramolecular structure and binding to the monomer in a binary complex. The amyloid-like shoulder at 550 nm suggests the former. Thus it seems that AmB has a

complementary face for both CR and amyloid.

One of the most significant findings in this report is that AmB can significantly delay the onset of fibrillization of A β 25–35 at near therapeutic levels of AmB (Figure 5). As this is one of the most toxic as well as one of the most fibrillization-prone fragments of the A β 1–42 peptide, this is a noteworthy result (37). The interference of amyloid formation by AmB suggests that AmB could either “cap” a growing fibril as has been proposed for N-methylated peptide β -sheet breakers (37) or could “overstabilize” the existing amyloid structure and thus slow the recruitment of new peptide units.

While AmB has never been investigated as a potential anti-Alzheimer’s drug, it has been studied for its antiprion effects for over 15 years (38). AmB and its more soluble, less toxic derivative MS-8209 have proven to be the most successful drugs for the treatment of experimental prion diseases in mouse and hamster model systems (7, 9, 39–43). Both MS-8209 and AmB are able to significantly delay the onset of scrapie in mice and hamsters and reduce the cerebral PrP_{res} load until the onset of the disease. These drugs are even effective when given 2 weeks prior to ic PrP_{res} inoculation and discontinued (39). Neither affects the spleen load of PrP_{res} to a great degree (9). Since these drugs were given via the ip route, it is clear that AmB and MS-8209 must affect either the entry into neural tissue or aggregation within the brain, in which case the drugs are somehow having an impact across the blood–brain barrier (44). As MS-8209 is less acutely toxic than AmB, it can be given in higher doses and is thus more effective (39). Despite this progress, it is still unclear what the exact molecular mechanism of these promising effects might be. Two major themes have emerged: blockage of formation or uptake of PrP_{res} or indirect clearance of PrP_{res} by AmB stimulation of macrophages (by an unknown mechanism) and increasing phagocytic clearance (44). This latter proposal has experimental support in that AmB has been shown to stimulate a primary response in macrophages and monocytes involving production of TNF- α and IL-1(5, 30, 45). Since macrophages are critical in sequestering PrP_{res} inocula and clearing the agent in animal systems, stimulation could be an important factor (46). However, AmB has also been shown to inhibit scrapie propagation in cultured cells in the absence of monocytes, and so there must also be a more direct mechanism (6, 47).

Like AmB, the anionic azo dye Congo Red has shown antiprion activity (9, 48) though it appears to be strain or species specific (9). In addition, CR inhibits both aggregation and toxicity of A β fibrils and aggregates (19, 20, 49, 50), and new CR derivatives have been investigated as Alzheimer’s therapies (51). Since CR binding is, in fact, diagnostic of amyloid and prion pathogenic structures, it is presumed that direct binding to misfolded proteins somehow inhibits propagation and/or damage due to misfolded assemblies (52). As AmB binds strongly to fibrillar peptides, a CR-like mechanism could be responsible for at least part of its effectiveness, though in the case of mouse scrapie disease CR and MS-8209 seem to have distinct mechanisms (9). In addition, inhibition of cellular damage by CR has been reported to be due to blockage of putative A β oligomer “protofibril” ion channels (53) or general inhibition of fibrillogenesis (49).

Another interesting implication of the strong interaction of AmB with amyloid structures could bear upon resistance and efficacy of AmB versus fungal pathogens. It has been recently shown that some fungi express a protein called hydrophobin which associates into CR-binding β -amyloid-like structures (54, 55). It is possible that such a protein could be a resistance factor for AmB if it sufficiently immobilizes the antibiotic. On the other hand, it could promote AmB sensitivity by sequestering AmB near the cell membrane. It will be interesting to see what, if any, effect of expression of this protein will have on AmB susceptibility.

With the realization that amyloid and prion diseases have much in common, including, apparently, infectivity (10), it seems plausible that similar therapeutic strategies could apply for both. In this report, we have established that AmB can interact specifically with amyloid folded proteins and can significantly inhibit fibril formation by one of the most potent and toxic of all fibril-forming peptides, A β 25–35. Though AmB itself and the commercial deoxycholate formulation (Fungizone) are too acutely toxic to contemplate as a therapeutic agent for long-term therapy of amyloid diseases, it is possible that one of many numerous, less toxic synthetic derivatives or AmB drug delivery systems could be part of a management strategy (7, 56). By analogy with promising anti-amyloid CR derivatives designed to cross the blood–brain barrier (51), such AmB derivatives may be worth investigating for Alzheimer’s and prion diseases.

ACKNOWLEDGMENT

We thank Emily Bauer and Evan Kwong for synthesis work and Kim Pierson for assistance with electron microscopy.

REFERENCES

- Hartsel, S., and Bolard, J. (1996) *Trends Pharmacol. Sci.* 17, 445–449.
- Croft, S. L., and Yardley, V. (2002) *Curr. Pharm. Des.* 8, 433–440.
- Konopka, K., Guo, L. S., and Duzgunes, N. (1999) *Antiviral Res.* 42, 197–209.
- Matsumoto, T., Kaku, M., Furuya, N., Usui, T., Kohno, S., Tomono, K., Tateda, K., Hirakata, Y., and Yamaguchi, K. (1993) *J. Antibiot. (Tokyo)* 46, 777–784.
- Rogers, P. D., Stiles, J. K., Chapman, S. W., and Cleary, J. D. (2000) *J. Infect. Dis.* 182, 1280–1283.
- Mange, A., Milhavel, O., McMahon, H. E., Casanova, D., and Lehmann, S. (2000) *J. Neurochem.* 74, 754–762.
- Demaimay, R., Adjou, K., Lasmezas, C., Lazarini, F., Cherifi, K., Seman, M., Deslys, J. P., and Dormont, D. (1994) *J. Gen. Virol.* 75, 2499–2503.
- Demaimay, R., Race, R., and Chesebro, B. (1999) *J. Virol.* 73, 3511–3513.
- Beringue, V., Adjou, K. T., Lamoury, F., Maignien, T., Deslys, J. P., Race, R., and Dormont, D. (2000) *J. Virol.* 74, 5432–5440.
- Lundmark, K., Westermark, G. T., Nystrom, S., Murphy, C. L., Solomon, A., and Westermark, P. (2002) *Proc. Natl. Acad. Sci. U.S.A.* 99, 6979–6984.
- Serpell, L. C., Sunde, M., and Blake, C. C. (1997) *Cell. Mol. Life Sci.* 53, 871–887.
- Serpell, L. C. (2000) *Biochim. Biophys. Acta* 1502, 16–30.
- Mudher, A., and Lovestone, S. (2002) *Trends Neurosci.* 25, 22–26.
- Baskakov, I. V., Legname, G., Baldwin, M. A., Prusiner, S. B., and Cohen, F. E. (2002) *J. Biol. Chem.* 277, 21140–21148.
- Armstrong, R. A., Lantos, P. L., and Cairns, N. J. (2001) *Neurosci. Lett.* 298, 53–56.
- Hardy, J., and Selkoe, D. J. (2002) *Science* 297, 353–356.
- Helmuth, L. (2002) *Science* 297, 1260–1262.

18. Howlett, D. R., Perry, A. E., Godfrey, F., Swatton, J. E., Jennings, K. H., Spitzfaden, C., Wadsworth, H., Wood, S. J., and Markwell, R. E. (1999) *Biochem. J.* 340, 283–289.
19. Abe, K., Kato, M., and Saito, H. (1997) *Neurosci. Res.* 29, 129–134.
20. Wood, S. J., MacKenzie, L., Maleeff, B., Hurler, M. R., and Wetzell, R. E. (1996) *J. Biol. Chem.* 271, 4086–4092.
21. Gordon, D. J., Sciarretta, K. L., and Meredith, S. C. (2001) *Biochemistry* 40, 8237–8245.
22. Kirkitadze, M. D., Bitan, G., and Teplow, D. B. (2002) *J. Neurosci. Res.* 69, 567–577.
23. Jobling, M. F., Huang, X., Stewart, L. R., Barnham, K. J., Curtain, C., Volitakis, I., Perugini, M., White, A. R., Cherny, R. A., Masters, C. L., Barrow, C. J., Collins, S. J., Bush, A. I., and Cappai, R. (2001) *Biochemistry* 40, 8073–8084.
24. Nielsen, L., Khurana, R., Coats, A., Frokjaer, S., Brange, J., Vyas, S., Uversky, V. N., and Fink, A. L. (2001) *Biochemistry* 40, 6036–6046.
25. Klunk, W. E., Jacob, R. F., and Mason, R. P. (1999) *Anal. Biochem.* 266, 66–76.
26. Ellison, D., Hinton, J., Hubbard, S. J., and Beynon, R. J. (1995) *Protein Sci.* 4, 1337–1345.
27. Bolard, J., Legrand, P., Heitz, F., and Cybulska, B. (1991) *Biochemistry* 30, 5707–5715.
28. Legrand, P., Romero, E. A., Cohen, B. E., and Bolard, J. (1992) *Antimicrob. Agents Chemother.* 36, 2518–2522.
29. Baas, B., Kindt, K., Scott, A., Scott, J., Mikulecky, P., and Hartsel, S. C. (1999) *Pharm. Sci. I*, U11–U32.
30. Hartsel, S. C., Baas, B., Bauer, E., Foree, L. T., Kindt, K., Preis, H., Scott, A., Kwong, E. H., Ramaswamy, M., and Wasan, K. M. (2001) *J. Pharm. Sci.* 90, 124–133.
31. Kowall, N. W., McKee, A. C., Yankner, B. A., and Beal, M. F. (1992) *Neurobiol. Aging* 13, 537–542.
32. Pike, C. J., Walencewicz-Wasserman, A. J., Kosmoski, J., Cribbs, D. H., Glabe, C. G., and Cotman, C. W. (1995) *J. Neurochem.* 64, 253–265.
33. Hartsel, S. C., Bauer, E. A., Kwong, E. H., and Wasan, K. M. (2001) *Pharm. Res.* 18.
34. Balbirnie, M., Grothe, R., and Eisenberg, D. S. (2001) *Proc. Natl. Acad. Sci. U.S.A.* 98, 2375–2380.
35. Malinchik, S. B., Inouye, H., Szumowski, K. E., and Kirschner, D. A. (1998) *Biophys. J.* 74, 537–545.
36. Tjernberg, L. O., Callaway, D. J., Tjernberg, A., Hahne, S., Lilliehook, C., Terenius, L., Thyberg, J., and Nordstedt, C. (1999) *J. Biol. Chem.* 274, 12619–12625.
37. Hughes, E., Burke, R. M., and Doig, A. J. (2000) *J. Biol. Chem.* 275, 25109–25115.
38. Pocchiari, M., Schmittinger, S., and Masullo, C. (1987) *J. Gen. Virol.* 68, 219–223.
39. Adjou, K. T., Demaimay, R., Lasmezas, C., Deslys, J. P., Seman, M., and Dormont, D. (1995) *Antimicrob. Agents Chemother.* 39, 2810–2812.
40. Adjou, K. T., Deslys, J. P., Demaimay, R., and Dormont, D. (1997) *Trends Microbiol.* 5, 27–31.
41. Adjou, K. T., Demaimay, R., Deslys, J. P., Lasmezas, C. I., Beringue, V., Demart, S., Lamoury, F., Seman, M., and Dormont, D. (1999) *J. Gen. Virol.* 80, 1079–1085.
42. Demaimay, R., Adjou, K. T., Beringue, V., Demart, S., Lasmezas, C. I., Deslys, J. P., Seman, M., and Dormont, D. (1997) *J. Virol.* 71, 9685–9689.
43. Adjou, K. T., Privat, N., Demart, S., Deslys, J., Seman, M., Hauw, J., and Dormont, D. (2000) *J. Comp. Pathol.* 122, 3–8.
44. Beringue, V., Lasmezas, C. I., Adjou, K. T., Demaimay, R., Lamoury, F., Deslys, J. P., Seman, M., and Dormont, D. (1999) *J. Gen. Virol.* 80, 1873–1877.
45. Rogers, P. D., Kramer, R. E., Chapman, S. W., and Cleary, J. D. (1999) *J. Infect. Dis.* 180, 1259–1266.
46. Beringue, V., Demoy, M., Lasmezas, C. I., Gouritin, B., Weingarten, C., Deslys, J. P., Andreux, J. P., Couvreur, P., and Dormont, D. (2000) *J. Pathol.* 190, 495–502.
47. Milhavet, O., Mange, A., Casanova, D., and Lehmann, S. (2000) *J. Neurochem.* 74, 222–230.
48. Caspi, S., Halimi, M., Yanai, A., Sasson, S. B., Taraboulos, A., and Gabizon, R. (1998) *J. Biol. Chem.* 273, 3484–3489.
49. Findeis, M. A. (2000) *Biochim. Biophys. Acta* 1502, 76–84.
50. Klunk, W. E., Debnath, M. L., Koros, A. M., and Pettegrew, J. W. (1998) *Life Sci.* 63, 1807–1814.
51. Lee, V. M. (2002) *Neurobiol. Aging* 23, 1039–1042.
52. Wille, H., Zhang, G. F., Baldwin, M. A., Cohen, F. E., and Prusiner, S. B. (1996) *J. Mol. Biol.* 259, 608–621.
53. Hirakura, Y., Yiu, W. W., Yamamoto, A., and Kagan, B. L. (2000) *Amyloid* 7, 194–199.
54. Butko, P., Buford, J. P., Goodwin, J. S., Stroud, P. A., McCormick, C. L., and Cannon, G. C. (2001) *Biochem. Biophys. Res. Commun.* 280, 212–215.
55. Mackay, J. P., Matthews, J. M., Winefield, R. D., Mackay, L. G., Haverkamp, R. G., and Templeton, M. D. (2001) *Structure (Cambridge)* 9, 83–91.
56. Graybill, J. R., Najvar, L. K., Fothergill, A., Hardin, T., Rinaldi, M., Lambros, C., and Regen, S. L. (1998) *Antimicrob. Agents Chemother.* 42, 147–150.

BI0270384